Benzene Oxidation in the Troposphere. Theoretical Investigation on the Possible Competition of Three Postulated Reaction Channels

Giovanni Ghigo and Glauco Tonachini*

Contribution from the Dipartimento di Chimica Generale ed Organica Applicata, Università di Torino, Corso Massimo D'Azeglio 48, 10125 Torino, Italy

Abstract: Three different attacks of $^3\Sigma_g$ O_2 on the hydroxycyclohexadienyl radical intermediate **I** (generated from the reaction of OH• with benzene) have been studied by Density Functional Theory. Both abstraction by O_2 of the hydrogen *gem* to OH in **I** (affording phenol) and O_2 addition to the π-delocalized system of **I** (producing a hydroxycyclohexadienyl peroxyl radical intermediate) appear to be very viable, with $\Delta H^{\ddagger} =$ 3−4 kcal mol^{-1}. The former reaction is exothermic by 27 kcal mol^{-1}, the latter only by 1 kcal mol^{-1}. In contrast, a recently repropounded pathway, which would lead to benzene oxide/oxepin, via hydrogen abstraction from the hydroxyl in **I** operated by O_2, appears not to be competitive, showing a significantly higher barrier ($\Delta H^{\ddagger} =$ 32 kcal mol^{-1}). Benzene oxide and oxepin are estimated to lie 21 and 19 kcal mol^{-1} above **I**, respectively.

Introduction

Aromatic hydrocarbons are commonly considered as one of the most important category of compounds implied in tropospheric oxidation. Among them, the most important are benzene and the methylated benzenes.[1] In the latter, H abstraction from CH$_3$ groups accounts for ca. 10% of the decay products, yielding benzaldehyde derivatives; this minor reaction channel does not appear to present particular mechanistic problems.[2,3] The prevalent reaction channel for benzene is believed to be the addition of OH• to the aromatic ring, yielding a hydroxycyclohexadienyl radical (**I** in Scheme 1). However, the subsequent degradation mechanisms are not well assessed and largely speculative.[1] Moreover, less than 50% of the initial carbon is generally accounted for in the experimentally observed products.[3]

As an example of the uncertainties still existing, it can be mentioned that recent experimental results indicate a rapid formation of HOO•,[4] which has been generally associated to phenol formation. Phenol can indeed result from either direct H abstraction operated by O_2 on **I** or HOO• elimination occurring in a peroxyl adduct of O_2 and **I**. However, HOO• could also form through different mechanisms not involving phenol. In fact, it has been recently postulated to derive from the formation of benzene oxide.[1] Still another possibility depends

Scheme 1

on prior NO reduction of peroxyl adducts obtainable at various stages of the degradation process of the aromatic, since H abstraction can subsequently be brought about by O_2 on the resulting oxy radicals, with carbonyl and HOO• formation (compare Figures 3 and 4 in ref 1 or Figure 1 in ref 5). As a
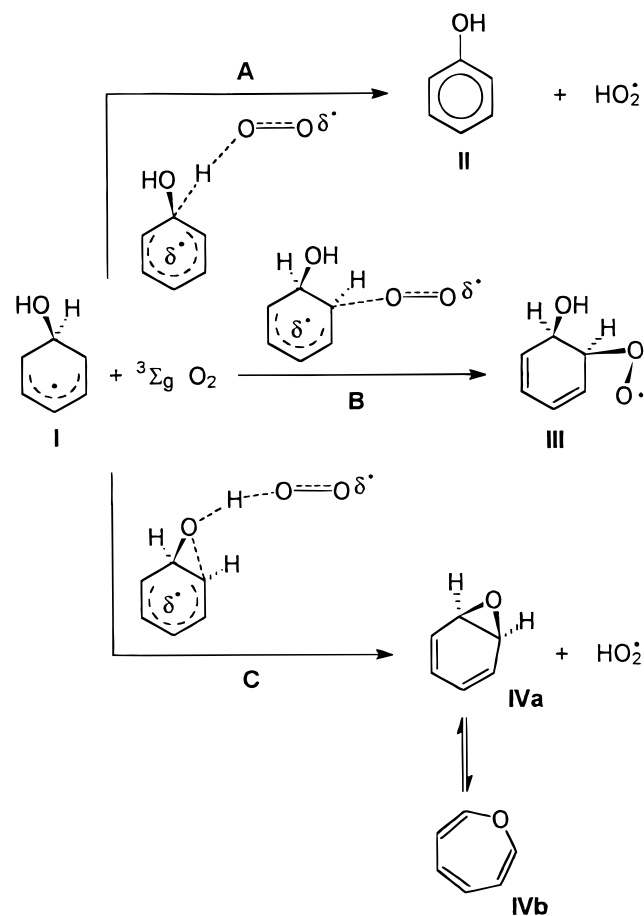
(1) Becker, K. H.; Barnes, I.; Ruppert, L.; Wiesen, P. Free Radicals in the Atmosphere: the Motor of Tropospheric Oxidation Processes. In *Free Radicals in Biology and Environment*; Minisci, F., Ed.; Kluwer Academic Publishers: Dordrecht, the Netherlands, 1997, Chapter 27, pp 365−385 and references therein. Grosjean, D. *Sci. Total Environ.* **1991,** *100,* 367−414.

(2) Atkinson, R. *J. Phys. Chem. Ref. Data* **1994,** Monograph No. 2; **1989,** Monograph No. 1.

(3) Atkinson, R. Reactions of Oxygen Species in the Atmosphere. In *Active Oxygen in Chemistry*; Valentine, J. S., Foote, C. S., Greenberg, A., Liebman, J. F., Eds.; Blackie Academic and Professional (Chapmann & Hall): New York, 1995; Chapter 7.

(4) Siese, M.; Koch, R.; Fittschen, F.; Zetzsch, C. Cycling of OH in the Reaction Systems Toluene/O$_2$/NO and Acetylene/O$_2$ and the Addition of OH to Isoprene. In *Transport and Transformation of Pollutants in the Troposphere. Proc. EUROTRAC Symp.* '94; Borrel, P. M., Borrel, P., Cvitas, T., Seiler, W., Eds.; SPB Academic Publishing bv.: The Hague, the Netherlands, 1994; pp 115−119.

further aspect of the problems involved in the interpretation of experimental outcomes, quite variable phenol yields (0 to 35% of the detected products) were reported in the literature.[5,6] This depends on the different experimental techniques, and is also likely to be due to the existence of parallel reaction pathways; it has indeed been shown to be dependent on the reaction conditions, within the same experiment.[7]

The atmospheric chemistry of benzene oxide/oxepin very recently has been studied experimentally.[5] The results collected in this research appear to be consistent with the variable phenol yields mentioned above and with the rapid release of HOO•. However, the formation itself of benzene oxide/oxepin has not been documented experimentally yet.

As regards the fate of the hydroxycyclohexadienyl radical initially formed, it has been found to react more rapidly with NO$_2$ than with O$_2$,[3,8] with rate constants that imply, on the basis of the relative abundance, that the latter reaction is however more important in the troposphere.[2] Yet, experiments carried out with variable [O$_2$]/[NO$_2$] ratios did not show changes in the yields of the more important products. This in turn would imply that rather similar product yields result from either reaction.

Recently, a study of the photochemical oxidation of benzene[9a] has been carried out by combining thermochemical group additivity rules[9b] and the semiempirical UHF/PM3 method. Reverse reactions were found to be important, and equilibrium was observed for both OH• addition to benzene and O$_2$ addition to the resulting adduct.

A recent theoretical study[10] has investigated the addition mechanisms of OH• and O$_2$ to methylated benzenes, as well as some exploration of NO$_2$ reactions of the initial hydroxyl adducts. This study has been carried out by initial semiempirical UHF/PM3 geometry optimizations, followed by DFT(B3LYP)/ 6-31G(d,p) single point energy calculations. While structures corresponding to energy minima were fully optimized, transition structures were located by an approximate procedure (a series of PM3 energy minimizations in correspondence of fixed values of a chosen parameter). For the addition of O$_2$ to four methylated hydroxycyclohexadienyl radicals, energy barriers ranging from 6.5 (*m*-xilene) to 8.6 (toluene) kcal mol^{-1} were estimated.

A previous theoretical study on toluene, carried out at the DFT level of theory,[11] had been focused on the identification of plausible reaction intermediates, on the basis of their relative stabilities (without reaction path study). Thus, 1-hydroxy-2-methylcyclohexadienyl radical was first identified as the most stable initial intermediate, followed by one peroxyl radical adduct among six considered, resulting from O$_2$ addition *ortho* to OH, and one subsequent (1,3)-peroxy-bridged intermediate among five examined, resulting from ring closure. Finally an epoxide structure was also explored, and found to be rather stable.

The aim of the present study is the assessment of the relative feasibility of the initial steps corresponding to three major channels that have been postulated in the literature (Scheme 1). These imply tranformations of the initial hydroxycyclohexadienyl radical intermediate **I** (generated from the reaction of OH• with benzene) operated by triplet O$_2$. Three reaction pathways are examined: two H-abstractions (A and C in Scheme 1) and one addition to the π-system (B). The study is carried out by determining the relevant transition structures (TS) and the corresponding intermediate products.

Method

The study of the model reactions discussed below was performed by determining, on the reaction energy hypersurfaces, the critical points corresponding to stable and transition structures. These were fully optimized by using gradient procedures[12] at the unrestricted DFT-(B3LYP) level of theory,[13] with the polarized split-valence shell 6-31G-(d) basis set,[14a] enriched with diffuse sp functions[14b] on the oxygen atoms, hereafter denoted as 6-31(+)G(d). In the study of pathways A and C, where transfer of one H takes place, a model test was conducted by adding p polarization functions to that H. This affected the relative energies in a nonnegligible way, but the TS geometry to a moderate extent. Therefore, the 6-31(+)G(d) optimum geometries were subsequently used in single-point energy evaluations with more extended basis sets. In the figures the more important optimum interatomic distances are reported in angstroms and angles in degrees. The nature of the critical points (energy minima, transition structures) was determined by diagonalization of the analytic Hessian (vibrational analysis). In two cases an Intrinsic Reaction Coordinate (IRC) analysis[15] was carried out, to unambiguously define the nature of the process to which the transition structures pertained. The energy differences relevant to the three reaction pathways were recomputed at the unrestricted DFT(B3LYP)/6-311+G(d,p) level,[14c] corresponding to the DFT(B3LYP)/6-31(+)G(d) optimized geometries. These unrestricted computations present moderate spin contaminations for the stable species, but depart significantly from the correct S^2 expectation value in the transition structures. These DFT doublet energies were corrected for spin contamination by the quartet, and triplet O$_2$ for the quintet, by using a formula analogous to that suggested by Yamaguchi.[16] These last corrected energy data were used in turn, in conjunction with the above-mentioned vibrational analysis data, to evaluate zero-point energies (ZPE) and thermal corrections to obtain activation and reaction enthalpies.[17] All calculations were carried out with the GAUSSIAN94 system of programs.[18] Geometry optimizations and analytic Hessian

(5) Klotz, B.; Barnes, I.; Becker, K. H.; Golding, B. T. *J. Chem. Soc., Faraday Trans.* **1997**, *93*, 1507−1516.

(6) Seuwen, R.; Warneck, P. *Int. J. Chem. Kinet.* **1995**, *28*, 315−332.

(7) Pan, X.-M.; Schuchmann, M. N.; von Sonntag, C. *J. Chem. Soc., Perkin Trans. 2* **1993**, 289−297. Fang, X.; Pan, X.; Rahmann, A.; Schuchmann, M. N.; von Sonntag, C. *Chem. Eur. J.* **1995**, *1*, 423−429.

(8) Knispel, R.; Koch, R.; Siese, M.; Zetzsch, C. *Ber. Bunsen-Ges. Phys. Chem.* **1990**, *94*, 1375−1379. In this paper the following Arrhenius expression was derived: k(O$_2$-adduct) = (6.9 × 10^{-15}) exp(−1040K/T) cm^3 s^{-1}.

(9) (a) Lay, T. H.; Bozzelli, J. W.; Seinfeld, J. H. *J. Phys. Chem.* **1996**, *100*, 6543−6554. (b) Benson, S. W. *Thermochemical Kinetics*; Wiley-Interscience: New York, 1976.

(10) Andino, J. M.; Smith, J. N.; Flagan, R. C.; Goddard, W. A., III; Seinfeld, J. H. *J. Phys. Chem.* **1996**, *100*, 10967−10980.

(11) Bartolotti, L. J.; Edney, O. E. *Chem. Phys. Lett.* **1995**, *245*, 119−122.

(12) Pople, J. A.; Gill, P. M. W.; Johnson, B. G. *Chem. Phys. Lett.* **1992**, *199*, 557−560. Schlegel, H. B. In *Computational Theoretical Organic Chemistry*; Csizsmadia, I. G., Daudel, Eds.; Reidel Publishing Co.: Dordrecht, the Netherlands, 1981; pp 129−159. Schlegel, H. B. *J. Chem. Phys.* **1982**, *77*, 3676−3681. Schlegel, H. B.; Binkley, J. S.; Pople, J. A. *J. Chem. Phys.* **1984**, *80*, 1976−1981. Schlegel, H. B. *J. Comput. Chem.* **1982**, *3*, 214−218.

(13) Parr, R. G.; Yang, W. *Density Functional Theory of Atoms and Molecules*; Oxford University Press: New York, 1989; Chapter 3. Becke, A. D. *Phys. Rev. A* **1988**, *38*, 3098−3100. Becke, A. D. *ACS Symp. Ser.* **1989**, *394*, 165. Pople, J. A.; Gill, P. M. W.; Johnson, B. G. *Chem. Phys. Lett.* **1992**, *199*, 557−560. Becke, A. D. *J. Chem. Phys.* **1993**, *98*, 5648−5652. Lee, C.; Yang, W.; Parr, R. G. *Phys. Rev. B* **1988**, *37*, 785−789.

(14) (a) Hehre, W. J.; Ditchfield, R.; Pople, J. A. *J. Chem. Phys.* **1972**, *56*, 2257−2261. Hariharan, P. C.; Pople, J. A. *Theor. Chim. Acta* **1973**, *28*, 213−222. (b) Diffuse functions: Clark, T.; Chandrasekhar, J.; Schleyer, P. v. R. *J. Comput. Chem.* **1983**, *4*, 294−301. (c) 6-311+G(d,p): Frisch, M. J.; Pople, J. A.; Binkley, J. S. *J. Chem. Phys.* **1984**, *80*, 3265−3269.

(15) Gonzalez, C.; Schlegel, H. B. *J. Chem. Phys.* **1989**, *90*, 2154−2161. Gonzalez, C.; Schlegel, H. B. *J. Phys. Chem.* **1990**, *94*, 5523−5527 and references therein.

(16) Yamanaka, S.; Kawakami, T.; Nagao K.; Yamaguchi, K. *Chem. Phys. Lett.* **1994**, *231*, 25−33. Yamaguchi, K.; Jensen, F.; Dorigo, A.; Houk, K. N. *Chem. Phys. Lett.* **1988**, *149*, 537−542. See also: Baker, J.; Scheiner, A.; Andzelm, J. *Chem. Phys. Lett.* **1993**, *216*, 380−388.

(17) (a) Reaction enthalpies were computed as outlined in: Foresman, J. B.; Frisch, Æ. *Exploring Chemistry with Electronic Structure Methods*; Gaussian, Inc.: Pittsburgh, PA, 1996; pp 166−168. (b) McQuarrie, D. A. *Statistical Mechanics*; Harper and Row: New York, 1976; Chapter 8.

Benzene Oxidation in the Troposphere

J. Am. Chem. Soc., Vol. 120, No. 27, 1998 6755

Table 1. Relative Energies (kcal mol^{-1}) of the Critical Points

	ΔE^a	ΔE^b	ΔE^c	ZPE^d	ΔH
benzene-OH + O$_2$	0.0	0.0	0.0	0.0	0.0
TS(A)	2.8	3.9	3.9	−0.5	2.8
phenol + HOO$^\bullet$	−26.9	−29.4	−27.7	0.6	−27.1
TS(B)	1.9	3.8	3.4	1.5	4.3
peroxy adduct	−8.2	−5.2	−3.4	3.0	−1.1
TS (C)	26.7	29.0	30.2	−1.3	32.1
benzene oxide + HOO$^\bullet$	16.9	19.2	20.9	0.1	21.0
oxepin + HOO$^\bullet$	17.1	16.9	18.6		

^{a} DFT(B3LYP)/6-31(+)G(d) spin contaminated ΔE values corresponding to optimized geometries. ^{b} DFT(B3LYP)/6-311+G(d,p) spin contaminated ΔE values obtained at the DFT(B3LYP)/6-31(+)G(d) optimized geometries. ^{c} Spin projected ΔE values. ^{d} Differential zero-point energy corrections computed at the DFT(B3LYP)/6-31(+)G(d) geometries.

computations were executed on IBM RISC/6000 550 and 360 computers (64 MB RAM both). A typical CPU timing for a single gradient on transition structure C (see below) was ca. 5 h; the frequency calculations on the same structure took 3 d 16 h. IRC computations were accomplished on a DEC Alpha 500/500 station (512 MB RAM), and required somewhat more than 14 h for six steps.

Results and Discussion

Three possibly competing reaction pathways were studied in their first step, to assess their relative feasibility (Scheme 1). All involve different reactions of $^3\Sigma_g$ O$_2$ with the hydroxycyclohexadienyl radical intermediate **I**, which is taken as the reference in reporting energy differences. The first two correspond to mechanisms postulated in the past years,[1] and begin either with the abstraction operated by O$_2$ of the hydrogen *gem* to OH in **I**, affording phenol (**II**, pathway A), or with O$_2$ addition to the π-delocalized system of **I**, producing a hydroxycyclohexadienyl peroxyl radical intermediate (**III**, pathway B). Both appear to be very viable, with energy barriers of 3−4 kcal mol^{-1} (Table 1). On the basis of the literature reports, the importance of the already mentioned reaction pathway A, leading to phenol, is controversial. In some studies large yields were reported,[6] but it seems quite dubious that this channel could generally prevail.[2] In this respect, it also appears interesting to consider the recent communication of Koch and Zetzsch on the oxidation of C$_6$D$_6$ by the OH radical, which yields mainly HO$_2$ and not DO$_2$, and seems to minimize the importance of pathway A.[19]

Pathway A. The transition structure corresponding to reaction A, TS(A), is reported in Figure 1. The transition vector (corresponding to an imaginary frequency of 449.4 cm^{-1}) is dominated by two contributions: the distance between the attacking oxygen and the hydrogen being abstracted (HO, coefficient 0.838) and the distance between this hydrogen and the tetracoordinated carbon (CH, coefficient −0.349). However, comparison with some results obtained by Ignatyev et al.[20] in a

(18) GAUSSIAN94: Frisch, M. J.; Trucks, G. W.; Schlegel, H. B.; Gill, P. M. W.; Johnson, B. G.; Robb, M. A.; Cheeseman, J. R.; Keith, T. A.; Petersson, G. A.; Montgomery, J. A.; Raghavachari, K.; Al-Laham, M. A.; Zakrzewski, V. G.; Ortiz, J. W.; Foresman, J. B.; Cioslowski, J.; Stefanov, B. B.; Nanayakkara, A.; Challacombe, M.; Peng, C. Y.; Ayala, P. Y.; Chen, W.; Wong, M. W.; Andres, J. L.; Replogle, E. S.; Gomperts, R.; Martin, R. L.; Fox, D. J.; Binkley, J. S.; Defrees, D. J.; Baker, J.; Stewart, J. P.; Head-Gordon, M.; Gonzalez, C.; Pople, J. A. Gaussian, Inc.: Pittsburgh, PA, 1995.

(19) Koch, R.; Zetzsch, C. Regeneration of HO$_2$ rather than DO$_2$ from Benzene-d_6−OH + O$_2$. In *Transport and Transformation of Pollutants in the Troposphere. Proc. EUROTRAC Symp.* '96; Borrel, P. M., Borrel, P., Cvitas, T., Seiler, W., Eds.; Computational Mechanics Publications: Southampton, UK, 1996.

(20) Ignatyev, I. S.; Yaoming, X.; Wesley, D. A.; Schaefer, H. F., III *J. Chem. Phys.* **1997**, *107*, 141−155.

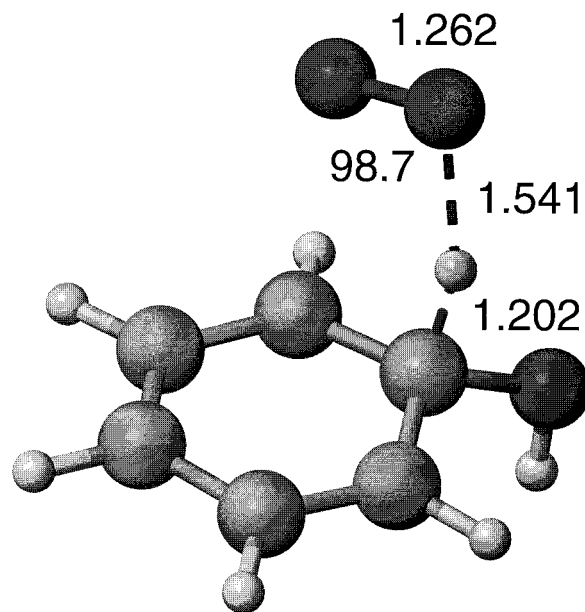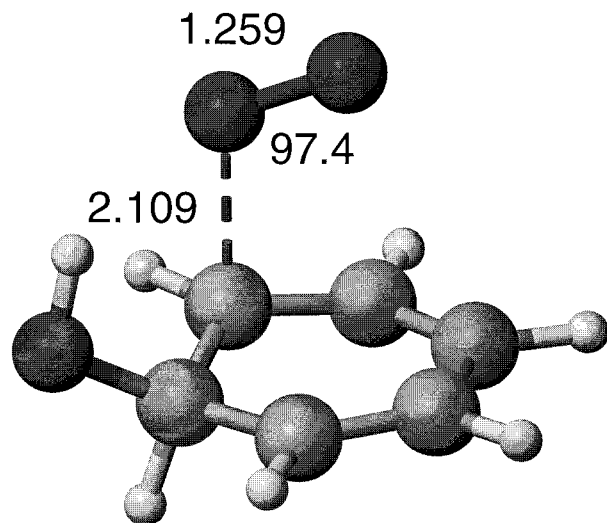**Figure 1.** Transition structure for hydrogen abstraction from the hydroxylated carbon in the hydroxycyclohexadienyl radical **I**, operated by O$_2$ and leading to phenol (reaction A).

theoretical study of the C$_2$H$_5$ + O$_2$ reaction could cast some doubts on the real nature of TS(A). In particular, the cis transition structure displayed in Figure 6 of ref 20, relevant to a concerted elimination process in the ethylperoxy radical, must be considered. It can suggest that the nature of TS(A) might as well be that of a transition structure for HOO$^\bullet$ elimination from one of the possible adducts of O$_2$ with **I** (namely, the one with O$_2$ bound to the ortho carbon, from the cycle face opposite to hydroxyl). Indeed, the distance of the terminal oxygen from the ortho carbon (OC) is not large, 2.44 Å, and compares with that of 2.20 Å, determined for elimination in the ethylperoxy radical.[20] To better assess if TS(A) is really relevant to the process of sheer H-abstraction from **I**, a standard IRC analysis[15] was carried out. This computation yields a series of steps, starting from the critical point, in a chosen direction. In the present case, the system was directed toward the still undetermined "reactant". On one hand, in both events (mere H-abstraction or concerted elimination), the system shift on the hypersurface would correspond to a lengthening of the HO distance and a shortening of the CH distance, because H-abstraction operated by one oxygen is part of the elimination process. On the other hand, the evolution of the suspicious OC distance, together with that of the OO bond length, could better help to clarify the matter. Indeed, if TS(A) were originating from a peroxyl adduct, OC should shorten (from 2.44 Å toward the adduct value of 1.50 Å), while the OO bond would be stretched out (the values of 1.26 Å in TS(A) and 1.32 Å in a peroxyl adduct provide a reference). In contrast, if TS(A) derived from the O$_2$ and I moieties, its OC and OO values should change in the opposite direction (OO = 1.215 Å in O$_2$). This test led to an unequivocal conclusion. As a result of a first series of twelve steps, OO underwent a shortening of 0.014 Å, corresponding to ca. 30% of the way toward the O$_2$ value. At the same time OC was elongated by 0.035 Å.

The changes in the geometrical parameters relevant to the H transfer in the transition state with respect to reagents and products can be defined as Δ and Δ', respectively. They suggest in the present case a fairly early transition structure, consistent with the significant exothermicity. In fact, ΔCH = +0.101 Å (+9%), while the O−H distance, 1.541 Å, is still larger than

Figure 2. Transition structure for O_2 addition to hydroxycyclohexadienyl radical **I**, leading to an ortho peroxyl radical adduct (reaction B).

the final one (0.983 Å in HOO$^\bullet$) by +57%. However, the change in OO bond length is significantly more advanced: the increase of 0.047 from the initial value of 1.215 Å in $^3\Sigma_g$ O_2 corresponds to 40% of the total change, being OO = 1.333 Å in HOO$^\bullet$. These variations describe a rather early and asynchronous process.

A second transition structure corresponding to pathway A was also determined. Its geometry (not reported in a figure) differs from the one just discussed primarily in that the OO bond is oriented in the opposite direction, away from the cycle. The geometrical parameters which depart more significantly from those of Figure 1 are: CH (1.180 Å) and HO (1.667 Å). Moreover, the terminal oxygen of the O_2 moiety interacts with the H in the hydroxyl group, at a distance of 2.002 Å. The energy of this structure with respect to **I** is 4.2 kcal mol^{-1}, to be compared with 2.8 kcal mol^{-1} for TS(A).

Pathway B. The addition pathway has already been considered in ref 10, by the procedure reported in the Introduction, for methylated benzenes but not for benzene itself. However, the energy barrier resulting from the complete DFT optimizations presented in this paper is significantly lower than those reported in ref 10. Kinetic data for O_2 addition to **I** in the gas phase[8] (and in aqueous solution[7]) have been reported in the last few years. Related data for structurally similar resonating radicals have also been discussed.[21] The transition structure corresponding to reaction B, TS(B), is reported in Figure 2.

The transition vector (corresponding to an imaginary frequency of 303.1 cm^{-1}) is dominated by a single contribution, the distance between the attacking oxygen and the carbon *ortho* to the tetracoordinated carbon (CO, coefficient 0.936 Å). The changes in the more important geometrical parameters are as follows: Δ'CO = 0.607 Å, which corresponds to a value larger than the final one by +40% (1.502 Å in the adduct **III**), ΔOO = 0.044 Å, and Δ'OO = 0.065 Å. The last values would indicate again a rather early transition structure. However, in this case, the reaction step exothermicity is much more modest (Table 1). This result is consistent with the reversibility of the addition process observed experimentally.[7,21]

Pathway C. The last process has been recently repropounded,[1] on the basis of the hypothesis put forward years ago by Shepson, Edney, and Corse.[22] This pathway would lead to

(21) Pan, X.-M.; Schuchmann, M. N.; von Sonntag, C. *J. Chem. Soc., Perkin Trans. 2* **1993**, 1021−1028. Porter, N. A. *Acc. Chem. Res.* **1986**, *19*, 262−268.
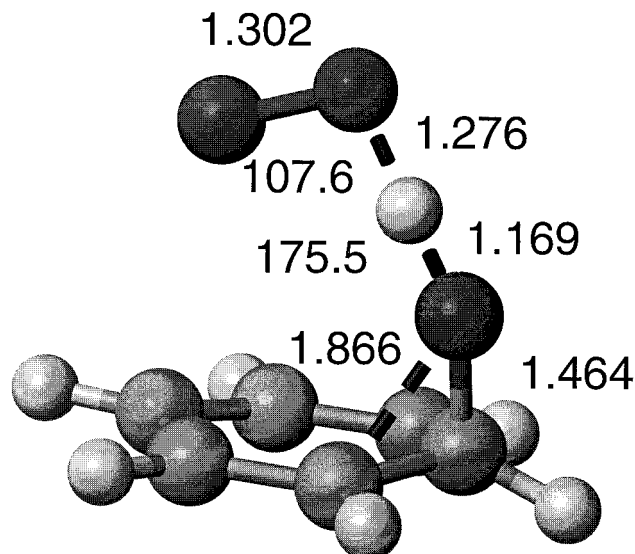

Figure 3. Transition structure for hydrogen abstraction from the hydroxyl group in the hydroxycyclohexadienyl radical **I**, operated by O_2. Closure of an epoxidic ring is concerted with this process, and leads to benzene oxide (reaction C).

the isomeric couple benzene oxide/oxepin (**IVa**, **IVb**), via hydrogen abstraction from the hydroxyl in **I** operated by O_2. The atmospheric chemistry of benzene oxide/oxepin very recently has been studied experimentally,[5] with very interesting results, in that this chemistry appears to be consistent with the variable phenol yields and with the rapid release of HOO$^\bullet$. However, as mentioned above, the formation itself of benzene oxide/oxepin has not been documented experimentally yet. Therefore, it is of some importance to assess if this isomeric couple is actually reachable in energy terms.

The transition structure corresponding to reaction C, TS(C), is reported in Figure 3. This structure describes a concerted process. In fact, as the hydroxyl hydrogen is transferred, the oxygen bound to the cycle bends toward the *ortho* carbon, to close an epoxidic cycle. The transition vector (corresponding to an imaginary frequency of 1384.3 cm^{-1}) is dominated by the following contributions: the distance between the attacking oxygen and the hydrogen being abstracted (HO, coefficient 0.527); the distance between this hydrogen and the oxygen bound to the cycle (OH, coefficient −0.497); and one planar and one dihedral angle, relevant to the hydroxyl oxygen, which describe together its bending toward the *ortho* carbon (−0.469 and −0.224, respectively). All these transition vector coefficients are again consistent with a concerted process. However, the variations in some important geometrical parameters suggest some asynchronicity in the transition structure for this concerted process. These are the previously defined Δ and Δ' of the parameters OO (in dioxygen and HOO radical), HO, and OH (relevant to H transfer), and the distance of the hydroxyl oxygen from the *ortho* carbon. Of these changes the following correspond to a rather late transition structure, and are consistent with the endothermicity of the reaction (Table 1): ΔOO = 0.081 Å, Δ'OO = 0.037 Å and ΔOC$_{ortho}$ = −0.573 Å, Δ'OC$_{ortho}$ = −0.426 Å. In contrast, it can be noted that in Figure 3: HO = 1.276 Å (Δ'HO = 0.293) and OH = 1.169 Å (ΔOH = 0.197). Thus, as mentioned above, the H transfer appears to be somewhat behind the other elementary processes, and suggests the idea of an asynchronous transition structure.

(22) Shepson, P. B.; Edney, E. O.; Corse, E. W. *J. Phys. Chem.* **1984**, *88*, 4122−4126.

As was the case for TS(A), some small but favorable interaction keeps the terminal oxygen of the O_2 moiety rather close to the ring carbons. The shortest distance is that with the para carbon (2.67 Å). An IRC analysis,[15] back in the direction of the "reactant", allows one to assess if TS(C) is really relevant to the O_2 H-abstraction process just described. Once again, if TS(C) were an hydroperoxyl elimination transition structure originating from a para peroxyl adduct, OC should shorten, tending to a value of ca. 1.50 Å, and the OO bond would undergo an elongation toward the value of 1.32 Å. In contrast, the result of a series of six steps shows OO undergoing a shortening of 0.029 Å, corresponding to ca. 62% of the way toward the O_2 value. At the same time OC was elongated by only 0.003 Å.

A search for a nonconcerted pathway leading to the same intermediate product was also attempted. Hydrogen abstraction from hydroxyl in a separate first step would produce a ylooxycyclohexadienyl diradical. To determine an approximate estimate of its energy, a triplet calculation was performed, assuming that the singlet would be located at a similar energy. The optimization resulted in an estimate of 53 kcal mol^{-1} (for the diradical plus hydroperoxyl radical) above the reagents, corresponding to ca. 26 kcal mol^{-1} above TS(C). This result ruled out any possible importance of a two-step diradical pathway.

Energetics. The energies relevant to the three pathways were refined by estimating the spin contamination for the single-point calculations with the more extended basis set. All energy minima show moderate contamination. The S^2 values are 2.0089 for $^3O_2$, 0.7854 for I, 0.7538 for HOO$^\bullet$, and 0.7545 for the $^3O_2$ adduct. The transition structures exhibit larger contaminations. The S^2 values are 0.9414 for TS(A), 0.9950 for TS(B), and 0.8066 for TS(C). This correction brings about small energy variations (Table 1), and the barriers of pathways A and B become slightly lower (by less than 0.1 and 0.4 kcal mol^{-1}, respectively). The barrier of pathway C is raised more substantially, yet only by 1.2 kcal mol^{-1}. The reaction energies

are also affected to a similar extent: pathways A and C by $+1.8$ kcal mol^{-1} and pathway B by $+2.1$ (the identical correction for pathways A and C is obviously due to the HOO radical).

A further refinement is then introduced by the computation of zero-point vibrational energies and enthalpies with the smaller basis set (Table 1). Also this correction does not alter substantially the overall picture obtained. Barrier A is lowered by 0.5 kcal mol^{-1}; barrier B is raised by 1.5 kcal mol^{-1}; and barrier C is lowered by 1.3 kcal mol^{-1}. The reaction energy A is affected to a very moderate extent ($+0.6$ kcal mol^{-1}) and reaction energy C is almost unmodified ($+0.1$). The largest correction is found for the O_2 adduct ($+3.0$ kcal mol^{-1}). The final estimate of the enthalpy differences for the three reactions (column 5) associates these values to the energy differences computed with the largest basis set.

In conclusion, both energy barrier and endothermicity indicate that pathway C is not favored with respect to the previous two. These in turn present energy barriers of similar height (Table 1). It is apparent from these data that reaction A is not easily reversible, while B is. That oxygen addition was a reversible process that had already been observed in experimental studies, as mentioned in the Introduction.[23]

Supporting Information Available: Tables of DFT-(B3LYP) energies of critical points and vibrational frequencies (2 pages, print/PDF). See any current masthead page for ordering information and Web access instructions.

JA973956R

(23) MolMol 2.4: a program for display and analysis of macromolecular structures. Koradi, R.; Billeter, M.; Wütrich, K. *J. Mol. Graphics* **1996**, *14*, 51−55.